Bioanalytical Method Development and Validation of Corynantheidine, a Kratom Alkaloid, Using UPLC-MS/MS and its Application to Preclinical Pharmacokinetic Studies

Tamara I. King (Conceptualization) (Methodology) (Investigation) (Validation) (Formal analysis) (Writing - original draft) (Writing - review and editing), Abhisheak Sharma (Conceptualization) (Investigation) (Writing - review and editing) (Supervision), Shyam H. Kamble (Conceptualization) (Investigation) (Writing - review and editing), Francisco León (Resources) (Investigation) (Writing - review and editing), Erin C. Berthold (Investigation) (Writing - review and editing), Raluca Popa (Investigation), Orélia Cerlati (Investigation), Boone M. Prentice (Conceptualization) (Methodology) (Validation) (Resources) (Writing - review and editing), Lance R. McMahon (Writing - review and editing) (Funding acquisition) (Resources), Christopher R. McCurdy (Conceptualization) (Resources) (Writing - review and editing) (Supervision) (Project administration) (Funding acquisition), Bonnie A. Avery (Conceptualization) (Resources) (Supervision) (Project administration)

PII: S0731-7085(19)32291-5

DOI: https://doi.org/10.1016/j.jpba.2019.113019

Reference: PBA 113019

To appear in: *Journal of Pharmaceutical and Biomedical Analysis*

Received Date: 19 September 2019

Revised Date: 25 November 2019

Accepted Date: 27 November 2019

Please cite this article as: King TI, Sharma A, Kamble SH, León F, Berthold EC, Popa R, Cerlati O, Prentice BM, McMahon LR, McCurdy CR, Avery BA, Bioanalytical Method Development and Validation of Corynantheidine, a Kratom Alkaloid, Using UPLC-MS/MS and its Application to Preclinical Pharmacokinetic Studies, *Journal of Pharmaceutical and Biomedical Analysis* (2019), doi: https://doi.org/10.1016/j.jpba.2019.113019

Bioanalytical Method Development and Validation of Corynantheidine, a Kratom Alkaloid, Using UPLC-MS/MS and its Application to Preclinical Pharmacokinetic Studies

Tamara I. King[a], Abhisheak Sharma[a,b], Shyam H. Kamble[a,b], Francisco León[c], Erin C. Berthold[a], Raluca Popa[a], Orélia Cerlati[d], Boone M. Prentice[d], Lance R. McMahon[e], Christopher R. McCurdy[b,c*], and Bonnie A. Avery[a,b]

[a]*Department of Pharmaceutics, College of Pharmacy, University of Florida, Gainesville, FL, 32610, USA*

[b]*Translational Drug Development Core, Clinical and Translational Sciences Institute, University of Florida, Gainesville, FL, 32610, USA*

[c]*Department of Medicinal Chemistry, College of Pharmacy, University of Florida, Gainesville, FL, 32610, USA*

[d]*Department of Chemistry, University of Florida, Gainesville, FL, 32611, USA*

[e]*Department of Pharmacodynamics, College of Pharmacy, University of Florida, Gainesville, FL, 32610, USA*

[#]**Correspondence:**

Dr. Christopher R. McCurdy, Department of Medicinal Chemistry, University of Florida, Gainesville, FL 32610, USA. E-mail: cmccurdy@cop.ufl.edu Phone: +1 352 294 8691 Fax: +1 352 392 9455

Highlights

- A UPLC-MS/MS method was developed and validated for the quantification of corynantheidine
- Mass spectrometry imaging showed the distribution of corynantheidine in the whole rat brain
- Preclinical PK studies were performed for corynantheidine in Sprague Dawley rats

Abstract

Corynantheidine, a minor alkaloid found in *Mitragyna speciosa* (Korth.) Havil, has been shown to bind to opioid receptors and act as a functional opioid antagonist, but its unique contribution to the overall properties of kratom remains relatively unexplored. The first validated bioanalytical method for the quantification of corynantheidine in rat plasma is described. The method was linear in the dynamic range from 1 to 500 ng/mL, requires a small plasma sample volume (25 µL), and a simple protein precipitation method for extraction of the analyte. The separation was achieved with Waters BEH C18 2.1 x 50 mm column and the 3-minute gradient of 10 mM ammonium acetate buffer (pH = 3.5) and acetonitrile mobile phase. The method was validated in terms of accuracy, precision, selectivity, sensitivity, recovery, stability, and dilution integrity. It was applied to the analysis of the male *Sprague Dawley* rat plasma samples obtained during pharmacokinetic studies of corynantheidine administered both intravenously (I.V.) and orally (P.O.) (2.5 mg/kg and 20 mg/kg, respectively). The non-compartmental analysis performed in Certara Phoenix® yielded the following parameters: clearance 884.1 ± 32.3 mL/h, apparent volume of distribution 8.0 ± 1.2 L, exposure up to the last measured time point 640.3 ± 24.0 h*ng/mL, and a mean residence time of 3.0 ± 0.2 h with I.V. dose. The maximum observed concentration after a P.O. dose of 213.4 ± 40.4 ng/mL was detected at 4.1 ± 1.3 h with a mean residence time of 8.8 ± 1.8 h. Absolute oral bioavailability was 49.9 ± 16.4%. Corynantheidine demonstrated adequate oral bioavailability, prolonged absorption and exposure, and an extensive extravascular distribution. . In addition, imaging mass spectrometry analysis of the brain tissue was performed to evaluate the distribution of the compound in the brain. Corynantheidine was detected in the corpus callosum and some regions of the hippocampus.

Keywords: Kratom, Corynantheidine; UPLC-MS/MS; Alkaloid; *Mitragyna speciosa*; pharmacokinetics

Introduction

Mitragyna speciosa (Korth.) Havil, a member of the Rubiaceae family is commonly known as kratom, ketum, or biak-biak. It is native to the Southeast Asian countries of Thailand, Malaysia, Indonesia, Myanmar, and Papua New Guinea. The natives in these areas have consumed the leaves of *M. speciosa* for centuries to treat a variety of conditions such as fatigue, exhaustion, pain, opioid withdrawal, and opioid dependence [1, 2]. The emergence of kratom products in the

United States, however, has created a controversy amidst an ongoing opioid crisis. Many opioid users turned to kratom in hopes of alleviating the symptoms of chronic pain, as well as the dependence caused by the use of opioid medications [3]. In recent years, reports have surfaced describing serious adverse events and casualties linked to kratom use in the United States and the Western world [3-9]. Some studies have also described withdrawal symptoms caused presumably by the cessation of kratom use, indicating potential dependence to kratom in regular users [8, 10]. As a result, the legal status of kratom in the US has become a topic of discussion among the federal regulatory agencies such as the Drug Enforcement Administration (DEA) and the Food and Drug Administration (FDA) [7, 11]. However, placing kratom into Schedule I will severely limit the researchers' access to the plant in order to decipher all potential benefits and liabilities of kratom.

Currently sufficient information is not available in the scientific literature about the contribution of individual alkaloids to the overall pharmacological properties of kratom. In this regard, the most abundant and most studied kratom alkaloid, mitragynine (MG) (which only differs from corynantheidine by the addition of a 9-methoxy moiety) is reported to act as a partial agonist at μ-opioid receptors, as well as act at α_2-adrenergic receptors [7, 12]. A metabolite of mitragynine and a minor alkaloidal constituent of kratom, 7-hydroxymitragynine (7HMG), is a potent μ-opioid agonist. There are very few studies focusing on other kratom alkaloids, and the total pharmacology of the plant cannot be explained only by its most abundant alkaloid. Interactions between the alkaloids *in vivo* must be also considered.

For example, corynantheidine binding to μ-opioid receptors has been reported with activity as an antagonist as evidenced by the reversal of morphine-induced inhibition of twitch of the Guinea pig ileum [13]. This could be explained if corynantheidine is a partial agonist and could therefore serve as an antagonist of the effects of a higher efficacy agonist. Some *in vitro* metabolic stability and *in vivo* toxicity studies of corynantheidine were performed. Beckett *et al*. showed that the major metabolite of corynantheidine in rabbit liver microsomes is due to O-demethylation [14]. Toxicity studies were reported by Paris *et al*. in mice with corynantheidine (extracted from *Pseudocinchona africana*) administered subcutaneously, and the LD_{50} in mice was found to be 0.55 g/kg [15]. The same group also reported hypotensive effects of corynantheidine administered intravenously in rabbits; moreover, the alkaloid almost fully blocked hypertenisve effects of adrenaline in rabbits, when given intravenously at doses higher than 10 mg/kg [16]. The extent to which corynantheidine blocked the effects of adrenaline through functional (i.e., including actions of corynantheidine at non-adrenergic receptors) or competitive antagonism (*i.e.*, at adrenergic receptors) could not be determined from these data.

Additionally, subcutaneous administration of 15-20 mg/kg of corynantheidine in rabbits caused miosis, and when co-injected with 0.2 mg/kg adrenaline, prevented adrenaline-induced mydriasis [16]. Obeng *et al*. recently performed binding studies with corynantheidine (manuscript is currently under review) and showed that corynantheidine binds to κ- and μ-opioid receptors (with K_i ± SEM values of 1910 ± 45.0 and 118 ± 11.8 nM respectively), as well as α_{-1D} (K_i = 41.7 ± 4.7 nM) [17]. Based on the potential dual actions of corynantheidine at μ-opioid and adrenergic receptors, it can be hypothesized that this alkaloid is important in the pharmacological utility of kratom as an aid in opioid withdrawal. Currently FDA approved medications for opioid use disorder target both these receptor types.

There are several methods used for the LC-MS analysis of kratom alkaloids, but these mainly focus on the major components, such as MG, or its metabolite, 7HMG [18, 19]. There is a method designed for the simultaneous evaluation of the ten key kratom alkaloids in commercial and plant samples but it was not optimized for use in plasma or other biological samples due to a 22.5 minute long run time, therefore a new method had to be developed [6]. With the growing interest in individual alkaloids of kratom, it is important to be able to accurately quantify the presence of those minor alkaloids in biological matrices. In addition, qualitative mass spectrometry imaging experiments were performed to evaluate the distribution of corynantheidine into the brain following a single intravenous injection. By elucidating the pharmacological and pharmacokinetic properties of each alkaloid of interest, it will be possible to better understand how each constituent contributes to the effects of kratom as a whole, including the liabilities versus therapeutic effects of the components. To the best of our knowledge, this is the first study focusing on the development of a quantitative bioanalytical method that was successfully applied in the analysis of plasma samples from the first reported oral and intravenous pharmacokinetic studies in male *Sprague Dawley* rats. Additionally, this is the first mass spectrometry imaging study demonstrating the distribution of corynantheidine in the rat brain.

1. Materials and methods

2.1 Chemicals and reagents

Corynantheidine (Figure 1) was isolated and characterized through the method described by Sharma *et al.* [6]. The compound was shown to be >99% pure; its structure and purity were confirmed by ^{1}H, ^{13}C NMR, UPLC-Q-TOF, and UPLC-MS/MS [6].

Yohimbine hydrochloride was purchased from Selleckchem (Houston, TX, USA). All solvents were of LC-MS grade. Ammonium acetate, sodium heparin, acetic acid, isopropanol, acetonitrile, and methanol were purchased from Fisher Scientific (Fair Lawn, NJ, USA). Water (J.T. Baker) and heparinized blank rat plasma were purchased from VWR International (Suwanee, GA, USA). Sodium heparin coated blood collection vials and sterile blood collection tubing were obtained from BASi (West Lafayette, IN, USA).

1.2 Chromatography and mass spectrometry conditions

A Waters Acquity I-Class Ultra Performance Liquid Chromatography (UPLC™) coupled with a Xevo TQS Micro™ triple quadrupole mass spectrometer (MS/MS) was used for bioanalysis. The UPLC was equipped with a binary pump, a degasser, a 10 µL sample loop, a temperature-controlled sample manager kept at 10 °C, and a column oven kept at 50 °C. Separation was achieved on a Waters Acquity BEH C18 (2.1 x 50 mm, 1.7 µm) column. Mobile phase consisted of aqueous ammonium acetate buffer (10 mM, pH 3.5) (A-solvent) and acetonitrile (B-solvent). Gradient elution began with 80% A (v/v) until 0.5 min, gradient changed linearly to 50% A at 1 min and was held constant until 1.8 min. At 2 min A-solvent returned to 80% and allowed to re-equilibrate to initial conditions until 3 min. The flow rate was set at 0.35 mL/min. The sample injection volume was set to 1 µL in partial loop needle overfill (PLNO) mode. The weak wash consisted of acetonitrile, methanol, and water (1:1:2, %v/v/v) and was set to 2400 µL, the strong wash was made of equal parts of methanol, acetonitrile, water, and isopropanol (%v/v/v/v) containing 0.1% formic acid, and the total strong needle wash volume was set to 800 µL to prevent carryover, if any.

The analyte (corynantheidine) and the internal standard (IS, yohimbine) were detected by a mass spectrometer in positive electrospray ionization (ESI^+) using multiple reaction monitoring (MRM) mode. Monitored analyte transitions were *m/z* 369.2 > 144.0 and *m/z* 369.2 > 226.1 with the collision energies set at 36 and 24 V, respectively. Yohimbine was observed at *m/z* 355.2 > 212.1 with the collision energy set at 22 V. The source capillary voltage was set to 0.5 kV and the cone voltage was 60.0 V and 22.0 V for corynantheidine and yohimbine transitions, respectively. The desolvation temperature was set to 450 °C. Desolvation and cone gas flow rates were 900 and 50 L/h, respectively.

2.3 Stocks, calibration standards, and quality controls

Primary stock (PS) solutions of corynantheidine (1 mg/mL in acetonitrile) and IS

(yohimbine, 0.5 mg/mL in water and acetonitrile, 1:1, %v/v) were prepared by weighing appropriate amounts of the compounds and dissolving them in respective solvents; the stocks were later stored at -20°C. The PS were used to generate working stocks (WS) for the preparation of calibration standards (CS) and quality control (QC) samples. CS and QC were prepared daily by spiking blank rat plasma (23 µL) with appropriate WS (2 µL) to yield 25 µL plasma samples of the following concentrations of corynantheidine: 1, 10, 50, 100, 200, 300, 400, and 500 ng/mL. The QC samples were made at the lowest limit of quantification (LLOQ, 1 ng/mL), low (LQC, 3 ng/mL), medium (MQC, 250 ng/mL), and high (HQC, 450 ng/mL) concentrations of analyte. All WS were stored at 4 °C when not in use for no longer than one week.

2.4 Sample preparation

Plasma samples were thawed at room temperature and vortex-mixed using a BenchMixer® (San Francisco, CA, USA) for 10 min before analysis. A sample aliquot of 25 µL was transferred into a micro-centrifuge tube and quenched with 200 µL of acetonitrile containing 10 ng/mL of IS (quenching solution). The samples were vortexed for 10 min at 2500 rpm and later centrifuged at 15000 rcf and 4 °C for 10 min. After protein precipitation, 180 µL of supernatant were withdrawn, transferred into autosampler vials and assayed using UPLC-MS/MS system. Plasma samples that were expected to exceed the linearity range of the bioanalytical method, were diluted with blank rat plasma that was used to generate CS and QC up to 10X dilution. The CS, QC, and samples were processed on the same day and analyzed together.

2.5 Method validation

The method was validated according to the FDA guidelines for the bioanalytical method validation [20]. Each set consisted of blank, blank with IS, eight non-zero calibration standards, and QC samples at four concentrations (N = 6, each). The quantitative bioanalytical method was validated in terms of selectivity, specificity, sensitivity, dilution integrity, accuracy, precision, recovery, and stability.

2.5.1 Selectivity, specificity, and carryover

Selectivity and specificity were evaluated by analyzing blank plasma samples from six different rats. Blank and blank with IS were processed to assess for the presence and/or interference from any endogenous substances that could have eluted at the same retention times as the analyte and IS. The IS interference was evaluated by comparing

the IS response in blank and spiked samples, and the average response should not have exceeded 5%. Carryover was evaluated by running blank samples immediately following highest concentration samples. If any analyte was detected in those blanks, the response should not have exceeded 20% of LLOQ

2.5.2 Sensitivity

The LLOQ has to have signal-to-noise ratio of at least 10-to-1 with accuracy within 20% of nominal concentration and precision of 20% CV.

2.5.3 Accuracy and precision

Accuracy and precision were established at four different levels: LLOQ, LQC, MQC, and HQC with six replicates of each on three separate days. Accuracy and precision were calculated as %bias and %R.S.D, respectively. For accuracy and precision calculation, within and between run variability was assessed within 15% of acceptance criteria of nominal value for all the concentration except LLOQ (20%).

2.5.4 Extraction recovery

The method was validated for recovery efficiency of the analyte following protein precipitation. An analytical standard curve (AS) was prepared in acetonitrile and water (80:20, %v/v), and QC samples for recovery at four concentrations were prepared in plasma and processed as described in section 2.4. The percent recovery was calculated by quantifying the QC samples prepared in plasma to the calibration curve made of the AS.

2.5.5 Stability

Analyte stability in plasma was assessed by subjecting LQC and HQC samples (N=6, each) to conditions likely to arise during sample storage, processing, and analysis. LQC and HQC samples (N=6, each) were left at room temperature on the benchtop for 9 h for benchtop stability evaluation. For freeze-thaw stability, samples were prepared and placed in -20 °C freezer chamber. They were removed the following day, allowed to fully thaw and placed back in the freezer. The cycle was repeated a total of three times. The samples were then analyzed with a freshly prepared calibration curve. Autosampler stability was assessed by leaving the extracted samples at 10°C in the UPLC sample organizer up to 48 h and later assayed with a freshly prepared calibration curve.

Stock stability was assessed in PS and WS for 30 days and 7 days respectively.

2.5.6 Dilution integrity

Blank rat plasma was spiked to yield a final high concentration plasma of 1000 ng/mL. The high concentration plasma (HCP) was then diluted with blank rat plasma (BRP) at 5 µL HCP + 20 µL BRP, 2.5 µL HCP + 22.5 µL BRP, and 1 µL HCP + 24 µL BRP to yield dilution factors 5x, 10x, and 25x respectively Dilution factor was calculated as a ratio of aliquot of HCP to the total volume of diluted sample. Each dilution integrity level sample was replicated six times and analyzed with a freshly prepared calibration curve.

2.6 Pharmacokinetic (PK) studies

To evaluate the *in vivo* PK parameters of corynantheidine, preclinical PK studies were performed. Procedures were conducted in accordance with the protocol #201810535 approved by the University of Florida Institutional Animal Care and Use Committee (IACUC). Healthy male *Sprague Dawley* rats with pre-installed right jugular vein cannulas, and weights of 250 ± 25 g were obtained from Envigo (Indianapolis, IN, USA). Animals were housed in single occupancy ventilated cages at the University of Florida vivarium with *ad libitum* access to food and water. For the duration of the PK studies, animals were contained inside the Culex® automated blood drawing metabolic cages up to 24 h. Each cage was equipped with a mesh floor, urine and feces receptacle, a catheter for automated blood collection, and a refrigerated compartment for the storage of collected blood samples.

A dose of 2.5 mg/kg of corynantheidine was administered intravenously (I.V.) to four rats. The formulation was prepared by weighing an appropriate amount of corynantheidine hydrochloride and dissolving it in normal saline with 1% Tween-80 (v/v) to yield a 2.5 mg/mL solution of equivalent free base. Solution formulation was filtered through a 0.2 µm syringe filter (Millex®). The blood samples (100 µL) were collected at the following time points: pre-dose, 0.08, 0.25, 0.5, 0.75, 1, 2, 4, 8, 12, 18, and 24 h post-dose. For the *per os* (P.O.) PK study, four fasted (12-14 hours) rats were administered 20 mg/kg of corynantheidine *via* oral gavage. The suspension was prepared using the corynantheidine hydrochloride, 5 mg carboxymethyl cellulose and distilled water to yield a final concentration of 5.0 mg/mL of corynantheidine. The blood samples (100 µL) were collected via Culex® system at the same time points as the I.V. study with an additional sample draw at 0.17 h. The blood samples were centrifuged for 10 min at 2500 rcf, plasma was collected and stored at -80 °C until analysis. Formulations were also quantified for corynantheidine content, and exact doses were used in the PK parameters analysis.

2.7 . Imaging mass spectrometry

One naïve animal (control) and one dosed with 10 mg/kg corynantheidine I.V. were euthanized 30 minutes post-dose. The whole brains were immediately removed, rinsed with saline, and frozen in dry ice.

Transverse sections of rat brain were collected at 10 µm using a Leica CM 3050S Cryostat (Leica Biosystems, Wetzlar, Germany) with the chamber set to -24°C and the object set to -22°C. Sections were then thaw mounted onto indium tin oxide (ITO)-coated slides (Delta Technologies, Loveland, CO, USA). Corynantheidine standards were prepared by mixing 1:1 a solution of 40 mg/mL 2,5-dihydroxybenzoic acid (DHB, Sigma-Aldrich, St. Louis, MO, USA) in 30/70/0.1 acetonitrile/water/trifluoroacetic acid with a solution of 5 µM corynantheidine in 50/50 acetonitrile/water. MALDI spots were then prepared by manually depositing 1 µL of this mixture onto a tissue section (i.e., the dried-droplet method). For imaging experiments, a DHB matrix layer was applied to the slides using a custom-built sublimation apparatus (110°C, 12.5 minutes, <70 mTorr, resulting in ~3.5 mg DHB added to the slide) [21].

All experiments were performed on a 7T solariX FT-ICR mass spectrometer equipped with an Apollo II dual MALDI/ESI source and a dynamically harmonized ParaCell (Bruker Daltonics, Billerica, MA, USA). The MALDI source consists of a Smartbeam II Nd:YAG laser system (2 kHz, 355 nm). Images were acquired at a pixel spacing of 200 µm in both the x and y dimensions using a ~75-µm laser beam and a 200-µm Smart Walk (2000 laser shots). Continuous accumulation of selected ions (CASI) was employed to improve the sensitivity of the $[M+H]^+$ corynantheidine ion by setting the Q1 mass to *m/z* 369.6 and the mass window to 20 *m/z*. Data were collected from *m/z* 200 to 1,000 using a 0.2447 s time-domain transient length, resulting in a resolving power of ~34,000 at *m/z* 369.216.

2.8 . Data processing

2.8.1 Bioanalytical method

The calibration standards, QC, and test samples were processed using TargetLynx®, an application of MassLynx 4.1. The QC and test samples were quantified against the CS. The peak area of the analyte at various concentrations was divided by the peak area of the IS; and the resulting ratio plotted against nominal concentrations of the samples. The 1/x weighing was used to achieve best fit of CS. The equation of the line was used to quantify study samples. The linearity was assessed for the range of 1 to 500 ng/mL.

2.8.2 PK study samples

Following the quantification of the samples in TargetLynx, a plasma concentration vs. time curve was constructed in SigmaPlot® 12.0. The data were further subjected to a non-compartmental analysis using linear trapezoidal method in Phoenix®. The key PK parameters were calculated.

2.8.3. Brain imaging

Data analysis was performed using Compass DataAnalysis 5.0 (Bruker Daltonics, Billerica, MA) and ion images were visualized using FlexImaging 5.0 (Bruker Daltonics, Billerica, MA). Ion images are displayed without normalization and with interpolation. Following image acquisition, tissue sections were stained using hematoxylin and eosin (H&E) and scanned using Aperio Scanscope CS (Leica Biosystems, Buffalo Grove, IL) bright field whole slide scanner. The images were visualized with ImageScope.

3 Results and Discussion

3.1 UPLC-MS/MS optimization

The conditions for the separation of the compounds and detection using the triple quadrupole mass spectrometer were carefully selected. The autotune option of the IntelliStart™ was used to select the best ion transitions with the highest stability and intensity. Both negative and positive modes were evaluated, but ESI^+ mode showed better response. The representative chromatograms are shown in Figure 2.

During the analysis of the study plasma samples, a second peak was detected having the same precursor > product ion transitions as those of the IS, yohimbine, but eluting at a retention time distinctly different from yohimbine and corynantheidine (Figure 1 I, J). Having a very selective and sensitive method with reproducible retention times allowed us to accurately quantify the *in vivo* plasma samples by identifying the yohimbine peak based on its retention time. The chromatographic conditions were able to achieve full baseline separation of the isotopic compounds. The identity of the putative metabolite currently cannot be confirmed, but likely it is a product of loss of a methylene group, based on the mass difference (- 14 Da).

Blank without IS (A, B); blank with IS (C, D); LLOQ (1 ng/mL) (E, F); pre-dose sample of rat dosed 2.5 mg/kg I.V. (G, H); 2 h sample post-dose in a rat dosed I.V.

The chromatographic conditions, with modified solvent composition in wash conditions, were adopted from the method of Sharma *et al*. [6]. Initially, carryover was detected in blanks following high concentration samples, but was eliminated through increasing column re-equilibration time up to 1 min. Strong wash consisted of equal parts acetonitrile, water, methanol, and isopropanol with 0.1% formic acid, % v/v; weak wash was adjusted by increasing aqueous proportion 1:1:2 acetonitrile : methanol : water, %v/v [6]

3.2 Sample preparation and calibration range

The described bioanalytical method requires a low plasma volume (25 µL), which allows for more frequent serial sampling in rats to achieve the most informative concentration-time profile. A simple protein precipitation sample preparation reduces the number of steps, and therefore errors, associated with carrying out multi-step extraction procedures.

A benefit of this method is also a long linearity range of 1 to 500 ng/mL of corynantheidine. The coefficient of determination, R^2, was always above 0.99 for all runs and 1/x weighing was applied in TargetLynx® to achieve best fit.

3.3 Method validation

The bioanalytical method was successfully validated in accordance with the FDA guidelines [20].

3.3.1 Selectivity, specificity, and carryover

Selectivity and specificity were assessed in at least six different plasma sources, in spiked and blank samples. Blank samples did not show any interfering compounds, metabolites, or endogenous substances that could be assumed to be the analyte. Likewise, in spiked samples, the method was able to accurately quantify the concentrations within 20% of LLOQ and 15 % in LQC, MQC, and HQC. There was no carryover noted in the blank samples following high concentration samples.

3.3.2 Sensitivity, accuracy, precision

The LLOQ of this method was 1 ng/mL with the signal-to-noise ratio well exceeding the recommended 10:1. Accuracy and precision were evaluated on three different days, and the results are summarized in Table 1 for inter- and intra-day variability. The matrix effects accounted for 8.0 % CV in post-extraction spiked samples, which is not considered as a significant matrix effect [22].

[Table 1]. Accuracy, precision, and extraction recovery for corynantheidine in rat plasma (N= 6 at each concentration)

3.3.3 Stability

The analyte proved to be stable in conditions likely to be present during sample collection, storage, and processing (Table S1). All data is shown as mean % of nominal value ± S.D. Working stocks were stable in the fridge at 4°C for up to 7 days (93% ± 9 %). Plasma samples can be safely stored at room temperature on a benchtop up to 9 h (88% ± 6 %). Extracted plasma samples may remain in a refrigerated autosampler at 10 °C up to 48 h (96% ± 9%). Freeze-thaw stability studies showed the analyte stable up to two freeze-thaw cycles (96% ± 5%), but not as reproducible after 3 freeze-thaw cycles (98 % ± 25%). It is therefore advised to not re-freeze the plasma samples for more than two cycles.

3.3.4 Dilution integrity

High concentration samples showed reliable and reproducible results with 5x (86.6 % ± 6.6), 10x (105.9 ± 13.3), and 25x (107.4 ± 13.4) dilutions (average % nominal value ± R.S.D.)

3.4 Preclinical PK

The developed bioanalytical method was successfully applied to quantification of corynantheidine in rat plasma samples collected during PK studies. A low volume of plasma (25 µL) was needed for the analysis which allowed for a reduction in the blood collection volume of the animals without compromising the reliability of the concentrations of corynantheidine in plasma as shown in Section 3.3. Following the I.V. administration of corynantheidine, plasma concentration-time profile (Figure 3) demonstrated a bi-exponential decay. The P.O. concentration-time profile showed a graph consistent with the phenomenon of flip-flop kinetics, when the absorption rate is much slower than the elimination rate (Figure 3).

Pharmacokinetic parameters were calculated for both routes of administration in all animals (Table 2) using Phoenix 7.1. In both I.V. and P.O. routes of administration, corynantheidine content was quantifiable up to 24 h. It would be recommended to extend the PK study in the future to capture the elimination phase more accurately. Due to flip-flop kinetics patterns observed after P.O. administration, properly calculating elimination half-life for this route of administration was difficult; therefore the results for P.O. administration are

reported in terms of mean residence time. In addition, for the calculation of the absolute oral bioavailability, the area under the curve up to the last point was used for both I.V. and P.O. dosing routes.

[Table 2]. Pharmacokinetic parameters of corynantheidine in male *Sprague Dawley* rats[a]

It is evident from the results of the non-compartmental analysis of the I.V. data that corynantheidine exhibits a very large apparent volume of distribution indicating extravascular permeation. The clearance value also slightly exceeds that of rat hepatic blood flow (828 mL/h), indicative of additional extrahepatic clearance pathways, but whose contribution is likely not very substantial [23]. Relatively long mean residence time (MRT) in both routes of administration has been noted: 3.0 ± 0.2 hours I.V. and 8.8 ± 1.8 hours P.O. In comparison, in a previously published PK study done in male rats, the MRT after I.V. administration of 4 mg/kg of 7HMG was 70.9 ± 10 minutes [24]. In addition, MG MRT was shown to be 137 ± 18 (mean ± R.S.D.) after I.V. dosing of MG of 5 mg/kg [19].

The exact cause of the flip-flop kinetics phenomenon is unclear, but it is possible that the formulation itself (suspension) had caused slower release and absorption of the compound. The prolonged absorption could also be explained by the compound cycling between liver and the plasma as it is usually shown with enterohepatic circulation; however, the absence of secondary peaks in the I.V. profile makes this possibility less plausible. To further evaluate the reasons behind this, a different oral formulation should be tried (e.g. solution to simplify absorption) with lower compound concentration due to solubility concerns.

3.5 Distribution of corynantheidine in the brain

Corynantheidine was readily detected in the dosed rat brain tissue (Figure 4C). The high-resolution accurate mass capabilities of the FT-ICR MS platform allow for the identification of *m/z* 369.2176 as protonated corynantheidine (0.84 ppm). The absence of *m/z* 369.2176 from control tissue (Figure 4A) and detection of corynantheidine standard from tissue (Figure 4B) confirm this identification. Imaging mass spectrometry analysis revealed distinct distribution of corynantheidine in the dosed rat brain. Using the corresponding H&E stained tissue sections, the rat brain atlas [25] was used to identify these regions as the corpus callosum and parts of the hippocampus, such as the hippocampal commissure and the fimbria (Figure 4D). As expected, corynantheidine was not detected in the control rat brain. This information demonstrates that corynantheidine readily crosses the blood-brain barrier. In addition, the localization of corynantheidine in areas of the hippocampus suggests the possibility of it interacting with the receptors located in this area, such as μ- and δ- opioid

receptors [26], adrenergic (both α and β) [27, 28], and serotonin $5HT_{2A}$ receptors [29]. Furthermore, substance P receptors have been observed in both hippocampus and corpus callosum [30, 31], and corynantheidine was detected in those areas. It is unclear which receptors are unquestionably interacting with corynantheidine aside from opioid and adrenergic receptors, but this information provides clues to what other avenues should be explored. Furthermore, there could be indirect effects on other receptors in this region. Regardless, this data certainly provides the grounds for further research.

4 Conclusions

A fast, simple, and sensitive UPLC-MS/MS method was developed and validated in accordance with the FDA guidelines for the quantification of corynantheidine, a minor kratom alkaloid, with potential actions at opioid and adrenergic receptors. This method covers the dynamic range from 1 to 500 ng/mL, with a quick runtime of only 3 minutes, and a small sample volume of 25 µL. The sample preparation is done through protein precipitation without compromising the sensitivity of the method. The validated method was utilized in our laboratory for the quantification of the plasma samples obtained during a preclinical PK study of corynantheidine in male *Sprague Dawley* rats. Cl was determined to be 884.1 ± 32.3 mL/h, V_d of 8.0 ± 1.2 L in I.V. dosed animals, indicating an extensive tissue distribution and minor contribution of extrahepatic clearance. The calculated oral bioavailability was 49.9 ± 16.4 %. The plasma concentration-time profile in orally dosed animals showed flip-flop kinetics with absorption rate slower than the elimination rate. Corynantheidine was detected in both studies up to 24 hours post-dose. It is recommended to extend monitoring studies in the future past that time in order to properly capture the elimination phase, especially in the P.O. dosing route. It is possible that the flip-flop kinetics were the result of a formulation used for the study (a suspension); therefore, additional studies must be done to understand the influence of the formulation on the absorption profile of corynantheidine. A long MRT was detected exceeding those of MG and HMG. It could be speculated that the prolonged presence of corynantheidine in the systemic circulation could be facilitating opioid withdrawal due to antagonistic activity of corynantheidine at µ-opioid receptor [32]. However, the alkaloid content of corynantheidine in kratom is less than 1%, and its potency is not known. Therefore, whether the physiologically active concentrations of corynantheidine could be achieved or not with the consumption of kratom and its products is unclear. It was shown that corynantheidine

crosses the blood-brain barrier and enters the corpus callosum and parts of hippocampal regions in the rat brain, as was shown with imaging mass spectrometry experiments. This study was the first evaluating preclinical PK in plasma as well as the distribution and accumulation of the compound in the brain. The information obtained from these studies will facilitate the future research into uncovering the properties of corynantheidine and its contribution to the pharmacology of kratom.

author statement

Tamara I. King: Conceptualization, Methodology, Investigation, Validation, Formal analysis, Writing – Draft, Review & Editing; **Abhisheak Sharma**: Conceptualization, Investigation, Writing – Review & Editing, Supervision; Shyam H. Kamble: Conceptualization, Investigation, Writing – Review & Editing; **Francisco León**: Resources, Investigation, Writing – Review & Editing; **Erin C. Berthold**: Investigation, Writing – Review & Editing; **Raluca Popa**: Investigation; **Orélia Cerlati**: Investigation; **Boone M. Prentice**: Conceptualization, Methodology, Validation, Resources, Writing – Review & Editing; **Lance R. McMahon**: Writing – Review & Editing, Funding Acquisition, Resources; **Christopher R. McCurdy**: Conceptualization, Resources, Writing – Review & Editing, Supervision, Project Administration, Funding acquisition; **Bonnie A. Avery**: Conceptualization, Resources, Supervision, Project Administration.

Declaration of interests

The authors declare that they have no known competing financial interests or personal relationships that could have appeared to influence the work reported in this paper.

The authors declare the following financial interests/personal relationships which may be considered as potential competing interests:

5 Acknowledgements

This study was supported by UG3 DA048353 grant from the National Institute on Drug Abuse and a generous donation through the University of Florida Foundation. Authors would also like to acknowledge startup funds through the University of Florida Department of Chemistry, College of Liberal Arts and Sciences, and Office of Research. The studies of Orélia Cerlati were sponsored by the National Science Foundation grant NSF CHE-1659782 through the REU

program.

6 References

[1] E.W. Boyer, K.M. Babu, J.E. Adkins, C.R. McCurdy, J.H. Halpern, Self-treatment of opioid withdrawal using kratom (*Mitragynia speciosa* korth), Addiction 103(6) (2008) 1048-1050.
[2] B. Vicknasingam, S. Narayanan, G.T. Beng, S.M. Mansor, The informal use of ketum (*Mitragyna speciosa*) for opioid withdrawal in the northern states of peninsular Malaysia and implications for drug substitution therapy, Int J Drug Policy 21(4) (2010) 283-288.
[3] E.W. Boyer, K.M. Babu, G.E. Macalino, W. Compton, Self-treatment of opioid withdrawal with a dietary supplement, Kratom, Am J Addict 16(5) (2007) 352-356.
[4] A.A. Philipp, M.R. Meyer, D.K. Wissenbach, A.A. Weber, S.W. Zoerntlein, P.G.M. Zweipfenning, H.H. Maurer, Monitoring of kratom or Krypton intake in urine using GC-MS in clinical and forensic toxicology, Anal Bioanal Chem 400(1) (2011) 127-135.
[5] T. Arndt, U. Claussen, B. Güssregen, S. Schröfel, B. Stürzer, A. Werle, G. Wolf, Kratom alkaloids and O-desmethyltramadol in urine of a “Krypton” herbal mixture consumer, Forensic Sci Int 208(1) (2011) 47-52.
[6] A. Sharma, S.H. Kamble, F. Leon, N.J. Chear, T.I. King, E.C. Berthold, S. Ramanathan, C.R. McCurdy, B.A. Avery, Simultaneous Quantification of Ten Key Kratom Alkaloids in *Mitragyna speciosa* Leaf Extracts and Commercial Products by Ultra-Performance Liquid Chromatography - Tandem Mass Spectrometry, Drug Test Anal (2019).
[7] W.C. Prozialeck, J.K. Jivan, S.V. Andurkar, Pharmacology of kratom: an emerging botanical agent with stimulant, analgesic and opioid-like effects, J Am Osteopath Assoc 112(12) (2012) 792-799.
[8] D. Singh, C.P. Müller, B.K. Vicknasingam, Kratom (*Mitragyna speciosa*) dependence, withdrawal symptoms and craving in regular users, Drug Alcohol Depend 139 (2014) 132-137.
[9] M.F. Neerman, R.E. Frost, J. Deking, A drug fatality involving Kratom, J Forensic Sci 58 (2013) S278-S279.
[10] L. McWhirter, S. Morris, A Case Report of Inpatient Detoxification after Kratom (*Mitragyna speciosa*) Dependence, Eur Addict Res 16(4) (2010) 229-231.
[11] W.C. Prozialeck, Update on the pharmacology and legal status of kratom, J Am Osteopath Assoc 116(12) (2016) 802-9.
[12] Z. Hassan, M. Muzaimi, V. Navaratnam, N.H. Yusoff, F.W. Suhaimi, R. Vadivelu, B.K. Vicknasingam, D. Amato, S. von Horsten, N.I. Ismail, N. Jayabalan, A.I. Hazim, S.M. Mansor, C.P. Muller, From Kratom to mitragynine and its derivatives: physiological and behavioural effects related to use, abuse, and addiction, Neurosci Biobehav Rev 37(2) (2013) 138-51.
[13] H. Takayama, H. Ishikawa, M. Kurihara, M. Kitajima, N. Aimi, D. Ponglux, F. Koyama, K. Matsumoto, T. Moriyama, L.T. Yamamoto, K. Watanabe, T. Murayama, S. Horie, Studies on the Synthesis and Opioid Agonistic Activities of Mitragynine-Related Indole Alkaloids: Discovery of Opioid Agonists Structurally Different from Other Opioid Ligands, J Med Chem 45(9) (2002) 1949-1956.
[14] A.H. Beckett, D.M. Morton, The metabolism of corynantheidine and 9-methoxycorynantheidine-type alkaloids by liver microsomes, Biochem Pharmacol 16(8) (1967) 1609-1615.
[15] R. Paris, M. Janot, R. Goutarel, Toxicite de la Corynantheidine, Nouvel Alcaloide Cristallise Des Ecorces De Pseudocinchoma-Africana Aug Chev, C R Seances Soc Biol Fil 139(7) (1945) 663-664.
[16] R. Paris, M. Janot, R. Goutarel, Sur Quelques Proprietes Physiologiques et en Particulier Articulier sur L’action Sympatholytique de la Corynantheidine, C R Seances Soc Biol Fil 139(7) (1945) 665-666.
[17] S. Obeng SHK, M. E. Reeves, L. F. Restrepo, N. J.-Y. Chear, S. Ramanathan, A. Sharma,

F. León, T. Hiranita, B. A. Avery, L. R. McMahon, and C. R. McCurdy. Investigation of the Adrenergic and Opioid Binding affinities, Metabolic Stability, and Plasma Protein Binding Properties of Selected In-dole-based Kratom Alkaloids. [Research Article]. In press 2019.
[18] P.K. Vuppala, S.P. Boddu, E.B. Furr, C.R. McCurdy, B.A. Avery, Simple, Sensitive, High-Throughput Method for the Quantification of Mitragynine in Rat Plasma Using UPLC-MS and Its Application to an Intravenous Pharmacokinetic Study, Chromatographia 74(9) (2011) 703.
[19] R. Kikura-Hanajiri, M. Kawamura, T. Maruyama, M. Kitajima, H. Takayama, Y. Goda, Simultaneous analysis of mitragynine, 7-hydroxymitragynine, and other alkaloids in the psychotropic plant “kratom” (*Mitragyna speciosa*) by LC-ESI-MS, Forensic Toxicol 27(2) (2009) 67-74.
[20] FDA, Guidance for Industry Bioanalytical Method Validation. US Department of Health and Human Services, Center for Drug Evaluation and Research (Ed.) Rockville, MD, 2018.
[21] J.A. Hankin, R.M. Barkley, R.C. Murphy, Sublimation as a method of matrix application for mass spectrometric imaging, J Am Soc Mass Spectrom 18(9) (2007) 1646-1652.
[22] P.J. Rudzki, E. Gniazdowska, K. Buś-Kwaśnik, Quantitative evaluation of the matrix effect in bioanalytical methods based on LC–MS: A comparison of two approaches, J Pharm Biomed Anal 155 (2018) 314-319.
[23] Davies, T. Morris, Physiological parameters in laboratory animals and humans, Pharm Res 10(7) (1993) 1093-1095.
[24] P.K. Vuppala, S. Jamalapuram, E.B. Furr, C.R. McCurdy, B.A. Avery, Development and validation of a UPLC-MS/MS method for the determination of 7-hydroxymitragynine, a μ-opioid agonist, in rat plasma and its application to a pharmacokinetic study, Biomed Chromatogr 27(12) (2013) 1726-1732.
[25] C. Watson, G. Paxinos, The rat brain in stereotaxic coordinates, Academic press San Diego, CA;1986.
[26] R. Quirion, J. Zajac, J. Morgat, B. Roques, Autoradiographic distribution of mu and delta opiate receptors in rat brain using highly selective ligands, Life Sci 33 (1983) 227-230.
[27] D.M. Perez, The adrenergic receptors: in the 21st century, Springer Science & Business Media 2006.
[28] R. Cash, R. Raisman, L. Lanfumey, A. Ploska, Y. Agid, Cellular localization of adrenergic receptors in rat and human brain, Brain Res 370(1) (1986) 127-135.
[29] T. Xu, S.C. Pandey, Cellular localization of serotonin2A (5HT2A) receptors in the rat brain, Brain Res Bull 51(6) (2000) 499-505.
[30] P. Barbaresi, Substance P receptor in the rat indusium griseum during postnatal development, Neurosci Res 130 (2018) 23-38.
[31] P. Barbaresi, E. Mensà, G. Bastioli, S. Amoroso, Substance P NK 1 receptor in the rat corpus callosum during postnatal development, Brain Behav 7(6) (2017) e00713.
[32] H. Takayama, Chemistry and pharmacology of analgesic indole alkaloids from the rubiaceous plant, *Mitragyna speciosa*, Chem Pharm Bull 52(8) (2004) 916-28.

[Figure 1]. Chemical structures of corynantheidine (I) and yohimbine (II; internal standard)

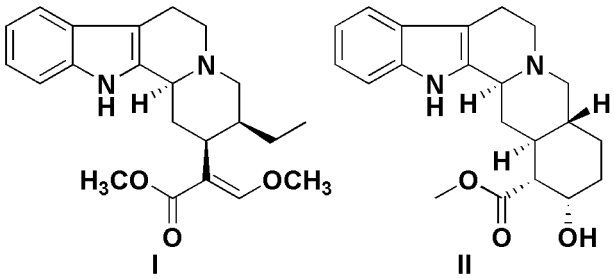

[Figure 2]. Representative chromatograms of corynantheidine (left panel) and IS (right panel):

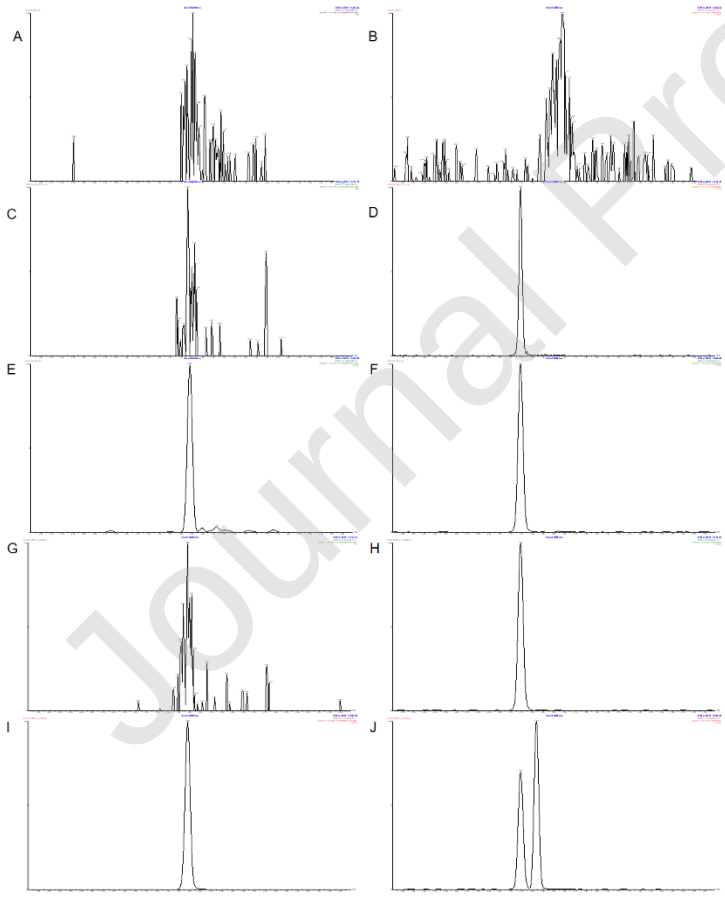

[Figure 3]. Mean plasma concentration-time profile of corynantheidine after 2.5 mg/kg I.V. (left) and 20 mg/kg P.O. (right) dose.

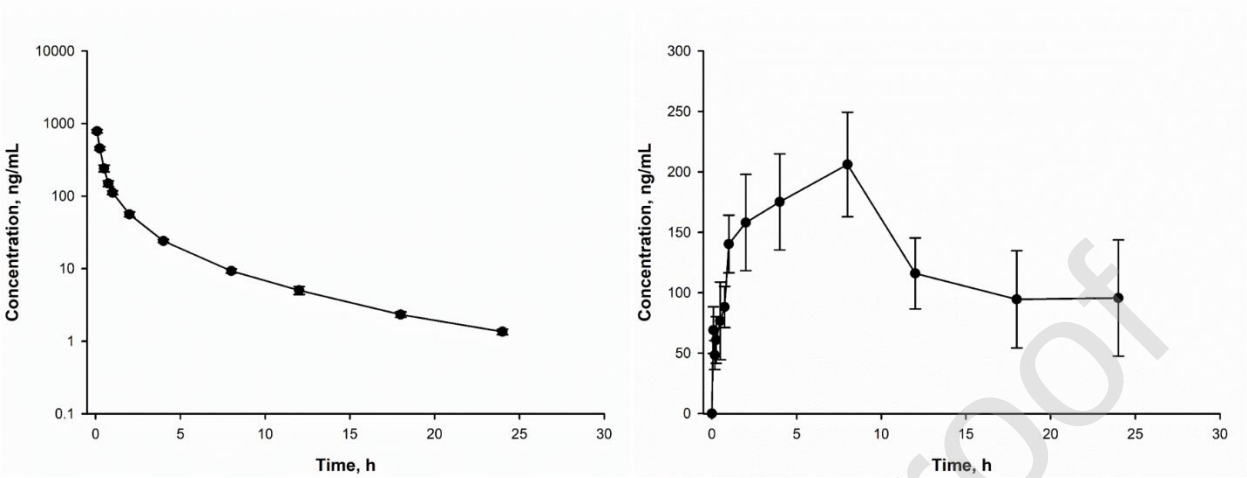

[Figure 4]. Distribution of corynantheidine in the rat brain.

A - control untreated brain section; B - control brain section spiked with standard corynantheidine; C - brain section, 10 mg/kg I.V., 30 min post dose; D, left - H&E stained dosed and control tissues; D, right – heat map of corynantheidine distribution in dosed and control sections respectively. Displayed mass spectra are the result of 10 spectral averages. Scale bar is 2 mm.

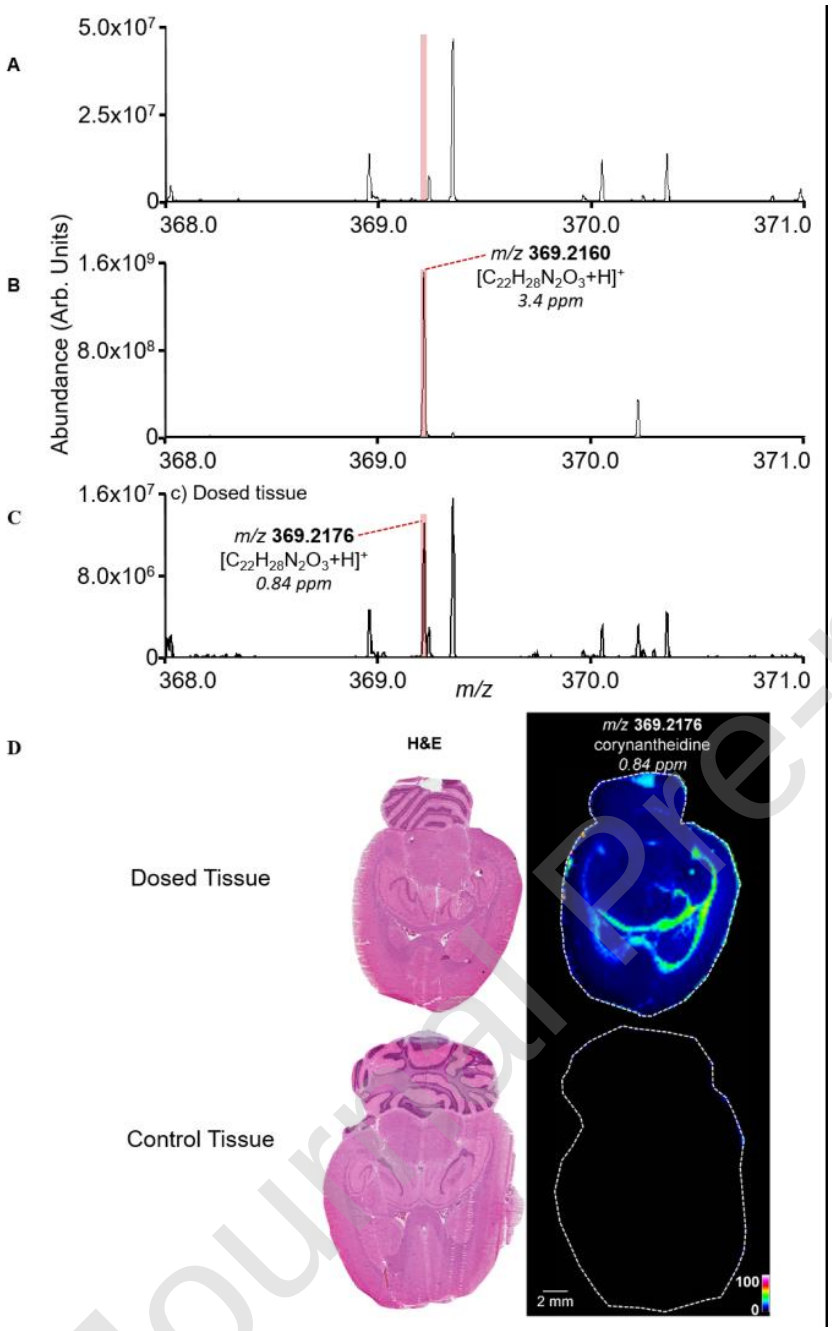

Table 1. Accuracy, precision, and extraction recovery for corynantheidine in rat plasma (N= 6 at each concentration)

Concentration	**Accuracy (% bias)**		**Precision (% R.S.D.)**		**Recovery (% Mean ± S.D)**
(ng/mL)	inter day	intra day	inter day	intra day	
1	-6.7	-7.4	12.8	11.1	81.1 ± 18.9
3	8.5	5.7	3.5	5.0	90.7 ± 9.3
250	-4.5	-2.8	7.3	3.5	84.3 ± 15.7
450	-0.3	2.7	6.9	8.6	85.1 ± 15.8

Table 2. Pharmacokinetic parameters of corynantheidine in male *Sprague Dawley* rats[a]

Parameters	**I.V.** **(2.5 mg/kg)**	**P.O.** **(20 mg/kg)**
C_{max} (ng/mL)	-	213.4 ± 40.4
T_{max} (h)	-	4.1 ± 1.3
K (1/h)	0.1 ± 0.0	-
$T_{1/2}$ (h)	6.9 ± 0.0	-
AUC_{inf} (h*ng/mL)	652.9 ± 23.3	-
AUC_{last} (h*ng/mL)	640.3 ± 24.0	2776.1 ± 910.6
CL (mL/h)	884.1 ± 32.3	1105.7 ± 613.3
V_d (L)	8.0 ± 1.2	9.2 ± 5.1
MRT (h)	3.0 ± 0.2	8.8 ± 1.8
F_{oral} (%)	-	49.9 ± 16.4

[a]*Values of pharmacokinetic parameters are mean ± S.E.M. (N= 4).*

K – elimination rate constant; $T_{1/2}$ – half-life; AUC_{inf} – total exposure extrapolated; AUC_{last} – total exposure up to the last measured time point; CL – clearance; V_d – apparent volume of distribution; MRT – mean residence time; C_{max} – maximum observed plasma concentration at time (T_{max}) observed; F_{oral} – absolute oral bioavailability